Optimization of Cellulose Nanocrystals from Ensete Ventricosum Pseudo Stem Fiber Using Response Surface Methodology

Abnet Mengesha Dube (abnetm817@gmail.com)
Wolkite University https://orcid.org/0000-0002-0901-5095

Research Article

Keywords: Response surface, Ensete Ventricosum, Hydrolysis, Cellulose Nanocrystals, Optimization, hydrolysis conditions

Posted Date: November 2nd, 2022

DOI: https://doi.org/10.21203/rs.3.rs-2009082/v1

Abstract

In the current world, cellulose is employed in many different applications to create cutting-edge materials like cellulose nanocrystals, which have numerous favorable uses in food packaging, medicine delivery, electronics, and many other fields. In this study, fibers from the *Ensete ventricosum* pseudo stem were hydrolyzed with sulfuric acid to produce cellulose nanocrystals. To get rid of non-cellulosic and amorphous components, mechanical and chemical pretreatments like water soaking, dewaxing, alkali treatment, and bleaching were carried out. The yield as responses was used to optimize the operation conditions of cellulose nanocrystals extraction from *Ensete ventricosum* pseudo stem fiber using Response Surface Methodology. The maximum production of cellulose nanocrystals is 39.49 percent with a crystallinity index of 69.7 percent under optimal hydrolysis conditions of 49 percent sulfuric acid concentration, 52°C hydrolysis temperature, and 36 minutes of hydrolysis time. The correctness of the results and the optimization technique itself have both been validated. Consequently, CNCs from EVPSF have potential use in a variety of fields with added value.

1. Introduction

The plant *Ensete ventricosum*, often known as the false banana, is a member of the genus Ensete, family Musaceae Ensete, and order Scitamineae [1]–[5]. This plant is commonly grown in sub-Saharan, central, and eastern Africa. And in the southern, south-western, and central regions of Ethiopia, it is one of the staple food crops eaten by about 20% of the population [1], [5]–[8]. *Ensete ventricosum* is a plant that is commonly farmed for food, and the procedures involved in its cultivation and food preparation generate enormous amounts of lignocellulose biomass waste [1], [3]. The pseudo-stem (a bundle of fibers) and leaves of the plant are the main sources of these residual wastes [3], [9]–[11]. The leaf lamina, leaf midribs, pseudo stem, and corm are the four fractional portions that make up the majority of *Ensete ventricosum's* dry matter [3]. According to studies, these dry substances are composed of the following percentages: leaf lamina 15–17 percent, pseudo stem 45–51 percent, stalk 9–11 percent, and corm 26–29 percent [3], [10], [12], [13]. One of the plant's parts, the *Ensete ventricosum* pseudo stem, has a great deal of potential for producing natural fibers for various applications by removing the undesirable components (hemicellulose 22.13–27.9, lignin as 6.88 ± 0.55–10.53 percent, and other trace amounts of impurities) for particular uses [9], [14]. Lignin, hemicellulose, wax, extractive, and other undesirable components of the pseudo-stem fiber must therefore be removed in order to produce cellulose nanocrystals.

Cellulose nanocrystals (CNCs) are cellulose derivatives that are extremely crystalline nanoparticles with dimensions in the nanometer range, widths ranging from 2–30 nm, and lengths ranging from 100–300 nm [15]–[18]. Due to its intriguing features, CNCs stand out among cellulose nanoparticles as a material that is suitable for various nanotechnology applications [19], [20]. Due to their origin and nature, CNCs offer distinct and promising physical, chemical, and mechanical properties, including high surface area, high aspect ratio, high tensile strength, high stiffness, and high fracture toughness. They are also very biodegradable and have a lot of hydroxyl groups [21], [22]. As a result, CCNs have grown in popularity in a wide range of applications, including packaging, paper, paperboard, catalysis, food industries, and medical products [15], hygiene products, paints, cosmetics, optical, biosensors [23], and nanocomposite [24]–[26]. Also, in different domains of application, such as concrete, ceramics, plastics, etc., they are used as reinforcing elements to improve the mechanical properties of composite materials [27].

It is possible to isolate CNCs using lignocellulose biomasses, which are made up of cellulose, lignin, and hemicellulose. However, the direct use of these lignocellulose biomasses by bacteria and acid for CNC synthesis is exceedingly sluggish and ineffective because of their crystallinity and heterogeneity [19], [28]. Therefore, there should be a pretreatment process to eliminate undesirable components from particular lignocellulose biomasses before the isolation of CNCs. The extraction of CNCs can be facilitated by a number of preprocessing techniques [29]. Acid hydrolysis procedures are frequently utilized in the extraction of CNCs because they are suitable for cellulose hydrolysis and are simple to use [16]. To eliminate the amorphous cellulose areas, the pretreated cellulose materials are subjected to hydrolysis with a strong acid under tightly regulated conditions [30]. Because they are more sensitive to acid than the crystalline areas of cellulose, the low-density

amorphous regions of cellulose effectively hydrolyze [31]. Therefore, by breaking up the amorphous regions, which are glyosidic bond, crystallites are freed from cellulose chain that has been subjected to acid treatment [21]. A variety of acids have been used to extract CNCs, with hydrochloric acid, phosphoric acid, and sulfuric acid being the principal ones [27]. For isolating CNCs, mineral acid hydrolysis is more efficient and uses less energy [32], [33]. Sulfuric acid is the most preferred and often used acid for the acid hydrolysis extraction of CNCs because to its strong isolation capabilities, ability to create a stable colloidal structure, and esterification of hydroxyl groups by sulfate ions [34][35]. In general, cellulose sources, sulfuric acid concentration, hydrolysis time and temperature, acid to cellulose ratio, and mixing speed have a significant impact on the yield and characteristics of CNCs recovered from lignocellulose biomass cellulose by sulfuric acid hydrolysis [36]. The most researched conditions for sulfuric acid extractions include hydrolysis periods of 10 to 120 minutes, temperatures of 25 to 85°C, and acid concentrations of 30 to 65 weight percent [27], [30], [37]–[39].

Since there is presently almost no study using the cellulose of *Ensete ventricosum* pseudo stem fibers for the isolation of CNC for subsequently using in a wide range of application fields, this study focuses on transforming it into nano-scaled material, cellulose nanocrystals. The cellulose in *Ensete ventricosum* pseudo stem fiber was hydrolyzed with sulfuric acid to isolate CNC using the acid hydrolysis technique. The optimum conditions for CNC isolation from the cellulose of *Ensete ventricosum* pseudo stem fibers were determined through an analysis of the RSM optimization of the sulfuric acid hydrolysis process.

2. Materials And Methods

2.1. Materials

According to previously published research by Abnet Mengesha Dube [5], all substances and compounds were gathered and used.

2.2. Preparation of Cellulose

Based on previously done and published research by Abnet Mengesha Dube [5], all chemical and mechanical preparation, pretreatments, and sampling were carried out.

2.3. Isolation of CNC

Acid hydrolysis of the previously processed cellulose in the preceding phases produced cellulose nanocrystals. Based on various combinations of BBD results, the hydrolysis was conducted using sulfuric acid (H_2SO_4) concentrations ranging from 40 to 65 percent by weight, hydrolysis temperatures of 45 to 65°C, and a hydrolysis time of 30 to 90 minutes with vigorous stirring. The most important variables that were examined against CNC yield were reaction temperature, reaction duration, and acid concentration, which were chosen based on data from several studies of cellulose from various lignocellulose biomasses and one variable at a time. 20 mL of sulfuric acid at various concentrations were used during the procedure for every gram of the bleached Ensete ventricosum pseudo-stem fiber [40]. By adding ten times as much freeze-cooled distilled water, the hydrolysis process was promptly stopped [41], [42]. After the cellulose sample had undergone hydrolysis, it was rinsed many times to remove any remaining sulfuric acid before being centrifuged repeatedly at 4000 rpm for 20 minutes to bring the pH level back to neutral [40], [43]. The average outcomes of these studies, which were carried out in triplicate, were noted. To remove non-reactive sulfate groups, salts, and soluble sugars, the centrifugation process' precipitate was subsequently dialyzed with distilled water using a dialysis tube cellulose membrane (D9277) for five days [5], [40]. To obtain cellulose nanocrystals in powder form for the following characterization task, the dialysis process' precipitate was then ultrasonically treated for 10 minutes. To prevent bacterial development, a few drops of chloroform were added to the CNCs suspension before being freeze dried. The yield of each dried CNCs sample was then determined using Eq. (3.1) [5], [40], [44].

$$\%Yield = (\frac{W1}{W2}) * 100 \quad 2.1$$

Where W1 and W2 are, respectively, freeze-dried CNCs and bleached cellulose. The work of other scholars contributed to the validation of the overall acid hydrolysis process [33], [45]–[49].

2.4. Characterizations

2.4.1. X-ray diffraction (XRD) analysis

The integrated area of the XRD data was used to determine how much the crystallinity index of all samples of isolated cellulose nanocrystals changed. To assess the impact of these hydrolysis conditions on the crystallinity of the isolated cellulose nanocrystals, five samples were chosen at various acid concentrations, temperatures, and times (40, 55, 30; 49, 52, 36; 52.5, 55, 60; 65, 55, 30; and 65, 55, 90, respectively). For this analysis, a diffractometer (XRD-7000 X-RAY DIFFRACTOMETER, Shimadzu Corporation, Japan) was used to obtain X-ray diffraction patterns of all powder samples that were scanned at room temperature between 2θ with a diffraction angle in the range of 10° to 80° and a step size of 0.02°. The following formulae (Eq. 2.2) was then used to calculate the crystallinity index (percent CI) of the samples [5], [50], [51].

$$\%CI = \left(\frac{I200 - Iam}{I200}\right) * 100 \quad 2.2$$

Where I_{200} is the greatest value of 200 lattice that exhibits the total of the amorphous and crystalline regions, and I_{am} is the minimum value between 110 and 200 lattice diffractions that exhibit the amorphous region.

2.5. Optimization

The experiments created for the isolation of cellulose nanocrystals were determined after a number of preliminary and one variable at a time (OVAT) experiments were conducted. Design expert software was used to examine the impact of each parameter and how they interacted to affect the yield of cellulose nanocrystals. The ideal hydrolysis conditions, including sulfuric acid concentration (w/w percent), hydrolysis duration (minutes), and hydrolysis temperature (°C), were found using a response surface based on the Box-Behnken Design (BBD) method for the response of interest, or yield (w/w percent). The three variables, concentration of sulfuric acid (X_1), reaction temperature (X_2), and reaction time (X_3) were created as independent variables for the BBD techniques. Table 1 summarizes these three factors and ranges of their levels. The main goals of applying the response surface method were to quantitatively illustrate the interaction between regulated input parameters and the response (yield) that was affected by these process factors [52]. The influence of independent variables on the dependent variable, a yield of CNCs from Ensete ventricosum pseudo-stem fiber, can be expressed using a second-order polynomial equation and a quadratic model, as shown in Eq. (2.3):

$$Yield = \beta 0 + \sum_{i=1}^{3} \beta i Xi \ + \sum_{i=1}^{3} \beta ii Xi^2 \ + \sum_{i=1}^{3} \sum_{j=i+1}^{3} \beta ij Xi Xj \quad 2.3$$

Where X_i and X_j are independent variables, and β_0, β_i, β_{ii}, and β_{ij} are the regression constant coefficients for the intercept, linear, quadratic, and interaction effects, respectively.

The Design-Expert 11 software suite was used for modeling, design analysis, and optimization. The experiment's response (yield w/w percent) and the effects of independent factors were examined using an ANOVA with a 95% level of confidence. Table 1 summarizes the experiment number, parameters, and their combinations.

Table 1
Summary of the coded and uncoded levels of the independent variables and BBD

Name		Symbol	Variable level		
			Low (-)	Intermediate (0)	High (+)
Concentration (%)		X_1	40	52.5	65
Temperature (°C)		X_2	45	55	65
Time (minutes)		X_3	30	60	90
For the three independent variables and their combinations, BBD					
		Factor 1	Factor 2	Factor 3	
Std Order	Run Order	Concentration (w/w %)	Temperature (°C)	Time (minute)	Yield (w/w %)
6	1	65	55	30	
16	2	52.5	55	60	
2	3	65	45	60	
10	4	52.5	65	30	
9	5	52.5	45	30	
5	6	40	55	30	
3	7	40	65	60	
17	*8*	*52.5*	*55*	*60*	
1	9	40	45	60	
11	10	52.5	45	90	
4	11	65	65	60	
7	12	40	55	90	
8	13	65	55	90	
13	14	52.5	55	60	
15	15	52.5	55	60	
12	16	52.5	65	90	
14	17	52.5	55	60	

3. Results And Discussion

3.1. Isolation of CNCs

3.1.1. Physical Appearances

The color and volume of the suspension varied from one experimental condition to the next, as seen in Fig. 1, Fig. 2, and Fig. 3. Lower and upper levels of hydrolysis conditions have a lower yield of CNCs, as well as white and black colors were observed, respectively. The yield of CNCs was measured at two different hydrolysis conditions: the first hydrolysis condition

(40 percent weight, 30 minutes, and 45°C) and the last hydrolysis condition (90 minutes, 65°C, and 65 percent weight), where the yield was 16.36 percent weight. These were the lower yield limitations under the initial and final cellulose hydrolysis conditions. The hydrolysis conditions in the middle of the reaction produced a good yield and medium color. The sulfuric acid content, duration, and temperature variations throughout the hydrolysis process are what cause the change in color and the yield of cellulose nanocrystals.

3.2. Characterization of CNCs

3.2.1. X-ray diffraction Analysis

Table 2
XRD data from and isolated CNCs at different hydrolysis conditions.

Acid concentration (%)	40	49	52.5	65	65
Temperature °C	55	52	55	55	55
Time (min)	30	36	60	30	90
CI (%)	66.0 ± 0.04	69.70 ± 0.08	73.51 ± 0.03	79.52 ± 0.03	75.38 ± 0.013

Three major and three minor peaks exist at 2θ of the CNC's XRD pattern. Peaks were seen in the experimental data at around 15.74, 16.8, 22.65, and 43.98, 64.32, and 77.4 as it was depicted in Fig. 4 that were attributed to the $1\bar{1}0$, 110, 200, and 004 planes, respectively. Eq. 2.2 was used to obtain the crystallinity index, and Table 2 summarizes the CNC results. The outcomes show that the amorphous portion of the cellulose is successfully eliminated during the acid hydrolysis process. As the concentration of sulfuric acid increased with moderate hydrolysis temperature and duration, the high crystal recovery of CNC suggests that the amorphous region was hydrolyzed into sugars while the crystalline portion remained intact. Both the amorphous and crystalline sections of cellulose began to hydrolyze into sugars at a high sulfuric acid concentration, high enough (65%) at a high hydrolysis temperature and time (55 ℃ and 90 min, respectively). As can be seen in the table, the crystallite index afterwards started to decline.

3.3. Response surface methodology

3.3.1. Model fitting

Table 3 includes the regression coefficients as well as the Fisher value (F-value) and probability (p-value) of the model fitting. The fitness and significance of the model are described using the F-value and p-value. If the F-value is greater than the critical F-value at a level of 5%, statistical significance is considered. The p-value 0.05 also determines the relevance of each fitting parameter toward the response value. As independent variables for the acid hydrolysis process, the concentration of sulfuric acid, hydrolysis temperature, and duration are the significant parameters. Figure 5 illustrated the model fit of the hydrolysis process and as a result, Eq. (3.4) provides the mathematical model for the yield recovery of CNC:

$$\mathrm{Yield} = +38.46 - 0.60\mathrm{A} - 3.49\mathrm{B} - 3.30\mathrm{C} + 0.32\mathrm{AB} - 0.86\mathrm{AC} - 1.53\mathrm{BC} - 4.70\mathrm{A}^2 - 3.83\mathrm{B}^2 - 2.48\mathrm{C}^2 3.4$$

Making predictions about the reaction to specific levels of each factor is possible using the equation in terms of coded factors. By default, the factors' high levels are coded as + 1 and their low levels as -1. By contrasting the factor coefficients, the coded equation can be used to determine the relative importance of the elements.

Table 3
For the yield of CNC, as the response, regression coefficients, F-values, and p-values (significant levels) were summarized.

Parameters	Percent of CNCs' Yield (%CNCs)		
	Coefficient	F-value	P-value
Intercept	38.46		< 0.0001
A	-0.60	885.00	< 0.0001
B	-3.49	29899.42	< 0.0001
C	-3.30	26811.43	< 0.0001
AB	0.32	125.86	< 0.0001
AC	-0.86	909.08	< 0.0001
BC	-1.53	2858.54	< 0.0001
A^2	-4.70	28562.69	< 0.0001
B^2	-3.83	19013.92	< 0.0001
C^2	-2.48	7980.11	< 0.0001

A = sulfuric acid concentration (%); B = Temperature (℃); C = Time (min); AB = Sulfuric acid concentration and Temperature interaction; AC = Sulfuric acid concentration and Time interaction; BC = Temperature and Time interaction; A^2= [sulfuric acid concentration] ^{2}; B^2= [temperature] ^{2}; C^2= [time] ^{2}.

3.3.2. Effects of Parameters on the Yield of Cellulose Nanocrystals

The impacts of each independent variable, including cumulative and interaction effects among factors on the dependent variable of the study, CNCs' yield, were described using response surfaces plots. Here, a regression model for BBD that was created using the Design-Expert 11 program was used to explain the response surfaces.

Figure 7 displays the yield surface plots for CNCs. The impact of sulfuric acid concentration, hydrolysis time, and hydrolysis temperature on CNC yield is shown in Fig. 7a and b. It has been discovered that CNC yield varies greatly at different hydrolysis conditions. Typically, the yield increases steadily to its maximum as the acid concentration rises. As the acid concentration rises further, the yield percentage started to falls. Only specific concentrations of sulfuric acid can be used to dissolve the crystalline components of cellulose. This range's deviation has a considerable impact on the crystalline components of cellulose, resulting in a decrease in CNC yield. Sulfuric acid concentrations greater than or less than 49.1% reduce CNC yield. Reaction time and temperature had a greater impact on the yield. At first, it started to climb a little, but as reaction time and temperature increased to their maximums, the yield decreased. The extended reaction time allows the fiber to interact with the acid solution for a longer period of time, which could lead to more crystalline component breakdown. The CNC yield is greatest at about 36 minutes of hydrolysis time; at reaction times greater than or less than 36 minutes, the CNC yield drops. Due to enhanced kinetic energy, which aids the breaking of intra and intermolecular bonds in the crystalline section of cellulose, extreme hydrolysis temperatures result in a drop in the yield percentage. The CNC yield decreases at reaction temperatures greater than or less than 52°C, depending on the hydrolysis temperature. Additionally, model fitting results on the importance of all variables are validated using these plots and Fig. 5. These results were in line with other earlier investigations into various lignocellulose biomasses that had been documented and published [37], [53]–[55].

3.4. Validation

To validate the optimization results, the acid hydrolysis process was repeated three times under optimal conditions, as shown in the Table 4. Based on its optimum conditions, the yield of CNCs obtained was 39.48 ± 0.057% with a standard error of 0.044%. It indicates the high accuracy of the optimization result.

Table 4
Validation of optimized results

Response	Predicted Mean	Predicted Median	Observed	Std dev	n	SE pred	95% PI low	Data Mean	95% PI high
Yield	39.49	39.49	39.5	0.057	3	0.044	39.38	39.48	39.6

4. Conclusion

Ensete ventricosum pseudo stem fiber (EVPSF), a promising lignocellulose material with sufficient cellulose content but insufficient lignin and hemicellulose, was used in this work as the raw material for the manufacture of CNCs. The crystalline index of the CNC is good. A sulfuric acid concentration of 49.1, a hydrolysis period of 36 minutes, and a temperature of 52 C resulted in a yield of more than 39.45 percent. The crystals with an index greater than 69.7 were recovered in this CNCs isolation. Therefore, CNCs from EVPSF have a potential use in tissue engineering, emulsifiers, enzyme immobilization, composite materials, medication administration, and the transport of nanomaterials.

Declarations

Acknowledgements

I would like to express my greatest gratitude to my supportive and patient advisor, Girma Gonfa (Ph.D.), who has supported me throughout the journey of this research work. I would also like to thank all chemical engineering laboratory technicians and other supporting bodies of Addis Ababa Science and Technology University. I thank them for their fruitful support and kindness. Finally, I would like to thank my family and friends for supporting me during the compilation of this work.

Ethical Approval

This work is in compliance with ethical standards.

Competing interest statement

The author declares no conflict of interest.

Author contribution statement

Abnet Mengesha Dube was responsible for the experiment's conception and design, execution of all experiments, data analysis, and interpretation, as well as the first draft of the manuscript and tracking of all editing and publication procedures.

Funding statement

No specific grants from funding organizations in the public, private, or not-for-profit sectors were given to this research.

Data availability statement

The corresponding author will provide the data sets created during and/or analyzed during the current investigation upon reasonable request.

Additional information

There is no extra data available for this paper.

References

1. Yemata G (2020) “Ensete ventricosum: A Multipurpose Crop against Hunger in Ethiopia,” *Scientific World Journal*, vol. Hindawi Limited, 2020. doi: 10.1155/2020/6431849
2. Borrell JS et al (2019) Enset in Ethiopia: A poorly characterized but resilient starch staple. Ann Bot 123(5):747–766. doi: 10.1093/aob/mcy214
3. Nurfeta A, Eik LO, Tolera A, Sundstøl F (2008) Chemical composition and in sacco dry matter degradability of different morphological fractions of 10 enset (Ensete ventricosum) varieties. 146:55–73. 10.1016/j.anifeedsci.2007.12.003
4. Brandt S et al (1997) “The ‘ Tree against hunger,’”Enset based Agric. Syst. Ethiop., p.56,
5. Dube AM (2022) Isolation and characterization of cellulose nanocrystals from Ensete ventricosum pseudo-stem fiber using acid hydrolysis. Biomass Convers Biorefinery. doi: 10.1007/s13399-022-02987-z
6. Birmeta G, Bakeeva A, Passoth V (2019) Yeasts and bacteria associated with kocho, an Ethiopian fermented food produced from enset (Ensete ventricosum). Antonie Van Leeuwenhoek 112(4):651–659. doi: 10.1007/s10482-018-1192-8
7. Teli MD, Terega JM (2017) Chemical, Physical and Thermal Characterization of Ensete ventricosum Plant Fibre. Int Res J Eng Technol 04(12):67–75 [Online]. Available: www.irjet.net
8. Nurfeta A, Tolera A, Eik LO, Sundstøl F (2008) Yield and mineral content of ten enset (Ensete ventricosum) varieties. Trop Anim Health Prod 40(4):299–309. doi: 10.1007/s11250-007-9095-0
9. Berhanu H et al (Jul. 2018) Characterization of crop residues from false banana /ensete ventricosum/ in Ethiopia in view of a full-resource valorization. PLoS ONE 13(7). doi: 10.1371/journal.pone.0199422
10. Fekadu D, Ledin I (1997) Weight and chemical composition of the plant parts of enset and the intake and degradability of enset by cattle. 49:249–257
11. Tsegaye A, Struik PC (2001) Enset (Ensete ventricosum (Welw.) Cheesman) kocho yield under different crop establishment methods as compared to yields of other carbohydrate-rich food crops. Neth J Agric Sci 49(1):81–94. doi: 10.1016/S1573-5214(01)80017-8
12. Nurfeta A, Tolera A, Eik LO, Sundstøl F (2008) The supplementary value of different parts of enset (Ensete ventricosum) to sheep fed wheat straw and Desmodium intortum hay. Livest Sci 119:1–3. doi: 10.1016/j.livsci.2008.02.010
13. Mohammed B, Gabel M, Karlsson LM (2013) Nutritive values of the drought tolerant food and fodder crop enset. 8:2326–2333. 10.5897/AJAR12.1296
14. Teli MD, Terega JM (2017) “Chemical, Physical and Thermal Characterization of Ensete ventricosum Plant Fibre,”Int. Res. J. Eng. Technol., vol. 04, no. 12, [Online]. Available: www.irjet.net
15. Lin N, Dufresne A (2014) Nanocellulose in biomedicine: Current status and future prospect. Eur Polym J 59:302–325. doi: 10.1016/j.eurpolymj.2014.07.025
16. Morais JPS, Rosa MDF, De Souza Filho MDSM, Nascimento LD, Do DM, Nascimento, Cassales AR (2013) Extraction and characterization of nanocellulose structures from raw cotton linter. Carbohydr Polym 91(1):229–235. doi: 10.1016/j.carbpol.2012.08.010
17. Klemm D et al (2018) Nanocellulose as a natural source for groundbreaking applications in materials science: Today’s state. Mater Today 21(7):720–748. doi: 10.1016/j.mattod.2018.02.001
18. Flauzino Neto WP, Silvério HA, Dantas NO, Pasquini D (2013) Extraction and characterization of cellulose nanocrystals from agro-industrial residue - Soy hulls. Ind Crops Prod 42(1):480–488. doi: 10.1016/j.indcrop.2012.06.041
19. Habibi Y, Lucia LA, Rojas OJ (2010) Cellulose nanocrystals: Chemistry, self-assembly, and applications. Chem Rev 110(6):3479–3500. doi: 10.1021/cr900339w

20. Klemm D et al (2011) Nanocelluloses: A new family of nature-based materials. Angew Chemie - Int Ed 50:5438–5466. doi: 10.1002/anie.201001273
21. Brinchi L, Cotana F, Fortunati E, Kenny JM (2013) Production of nanocrystalline cellulose from lignocellulosic biomass: Technology and applications. Carbohydr Polym 94(1):154–169. doi: 10.1016/j.carbpol.2013.01.033
22. Leung ACW, Lam E, Chong J, Hrapovic S, Luong JHT (2013) Reinforced plastics and aerogels by nanocrystalline cellulose. 10.1007/s11051-013-1636-z
23. Nooredeen M (2019) Cellulose nanocrystals decorated with gold nanoparticles immobilizing GOx enzyme for non-invasive biosensing of human salivary glucose. 11. 10.1039/c9ay02176k. 48
24. Collazo-Bigliardi S, Ortega-Toro R, Chiralt Boix A (2017) "Isolation and characterisation of microcrystalline cellulose and cellulose nanocrystals from coffee husk and comparative study with rice husk," *Carbohydr. Polym.*, vol. 191, no. October pp. 205–215, 2018, doi: 10.1016/j.carbpol.2018.03.022
25. Johar N, Ahmad I, Dufresne A (May 2012) Extraction, preparation and characterization of cellulose fibres and nanocrystals from rice husk. Ind Crops Prod 37(1):93–99. doi: 10.1016/j.indcrop.2011.12.016
26. Lam E, Male KB, Chong JH, Leung ACW, Luong JHT (2012) Applications of functionalized and nanoparticle-modified nanocrystalline cellulose. Trends Biotechnol 30(5):283–290. doi: 10.1016/j.tibtech.2012.02.001
27. Dhar P, Bhasney SM, Kumar A, Katiyar V (2016) Acid functionalized cellulose nanocrystals and its effect on mechanical, thermal, crystallization and surfaces properties of poly (lactic acid) bionanocomposites films: A comprehensive study. Polym (Guildf). doi: 10.1016/j.polymer.2016.08.028
28. Harmsen P, Bermudez L, Bakker R (2010) "Literature Review of Physical and Chemical Pretreatment Processes for Lignocellulosic Biomass,"Onderzoek, [Online]. Available: www.wur.nl
29. Merklein K, Fong SS, Deng Y (2016) Biomass Utilization. Elsevier B V. doi: 10.1016/B978-0-444-63475-7.00011-X
30. Espino E, Cakir M, Domenek S, Román-gutiérrez AD, Belgacem N, Bras J (2014) Isolation and characterization of cellulose nanocrystals from industrial by-products of Agave tequilana and barley. Ind Crop Prod 62:552–559. doi: 10.1016/j.indcrop.2014.09.017
31. Lee J, Jeffries TW (2011) Efficiencies of acid catalysts in the hydrolysis of lignocellulosic biomass over a range of combined severity factors. Bioresour Technol 102(10):5884–5890. doi: 10.1016/j.biortech.2011.02.048
32. Frost BA, Johan Foster E (2020) Isolation of thermally stable cellulose nanocrystals from spent coffee grounds via phosphoric acid hydrolysis. J Renew Mater 8(2):187–203. doi: 10.32604/jrm.2020.07940
33. Mueller S, Weder C, Foster EJ (2014) Isolation of cellulose nanocrystals from pseudostems of banana plants. RSC Adv 4(2):907–915. doi: 10.1039/c3ra46390g
34. Dong XM, Revol JF, Gray DG (1998) Effect of microcrystallite preparation conditions on the formation of colloid crystals of cellulose. Cellulose 5(1):19–32. doi: 10.1023/A:1009260511939
35. Lu P, Lo Hsieh Y (2010) Preparation and properties of cellulose nanocrystals: Rods, spheres, and network. Carbohydr Polym 82(2):329–336. doi: 10.1016/j.carbpol.2010.04.073
36. Deepa B et al (2015) "Utilization of various lignocellulosic biomass for the production of nanocellulose: a comparative study," *Cellulose*, vol. 22, no. 2, pp. 1075–1090, doi: 10.1007/s10570-015-0554-x
37. Thambiraj S, Ravi Shankaran D (2017) Preparation and physicochemical characterization of cellulose nanocrystals from industrial waste cotton. Appl Surf Sci 412:405–416. doi: 10.1016/j.apsusc.2017.03.272
38. Elazzouzi-hafraoui S, Nishiyama Y, Putaux J, Heux L, Dubreuil F, Rochas C (2008) "The Shape and Size Distribution of Crystalline Nanoparticles Prepared by Acid Hydrolysis of Native Cellulose," pp.57–65,
39. Beck-candanedo S, Roman M, Gray DG (2005) "Effect of Reaction Conditions on the Properties and Behavior of Wood Cellulose Nanocrystal Suspensions," pp.1048–1054,

40. dos Santos RM, Flauzino Neto WP, Silvério HA, Martins DF, Dantas NO, Pasquini D (2013) Cellulose nanocrystals from pineapple leaf, a new approach for the reuse of this agro-waste. Ind Crops Prod 50:707–714. doi: 10.1016/j.indcrop.2013.08.049
41. Larissa LA, Fonsêca AF, Pereira FV, Druzian JI (2015) Extraction and characterization of cellulose nanocrystals from corn stover. Cellul Chem Technol 49(2):127–133
42. Martins DF et al (2015) The influence of the cellulose hydrolysis process on the structure of cellulose nanocrystals extracted from capim mombac ¸ a (Panicum maximum). Ind Crop Prod 65:496–505. doi: 10.1016/j.indcrop.2014.10.035
43. Oun AA, Rhim JW (2016) Isolation of cellulose nanocrystals from grain straws and their use for the preparation of carboxymethyl cellulose-based nanocomposite films. Carbohydr Polym 150:187–200. doi: 10.1016/j.carbpol.2016.05.020
44. Hemmati F, Mahdi S, Kashaninejad M, Barani M (2018) Synthesis and characterization of cellulose nanocrystals derived from walnut shell agricultural residues. Int J Biol Macromol 120:1216–1224. doi: 10.1016/j.ijbiomac.2018.09.012
45. Johar N, Ahmad I, Dufresne A (2012) Extraction, preparation and characterization of cellulose fibres and nanocrystals from rice husk. Ind Crops Prod 37(1):93–99. doi: 10.1016/j.indcrop.2011.12.016
46. Kallel F, Bettaieb F, Khiari R, García A, Bras J, Chaabouni SE (2016) Isolation and structural characterization of cellulose nanocrystals extracted from garlic straw residues. Ind Crops Prod 87:287–296. doi: 10.1016/j.indcrop.2016.04.060
47. Lu P, Lo Hsieh Y (Jan. 2012) Preparation and characterization of cellulose nanocrystals from rice straw. Carbohydr Polym 87(1):564–573. doi: 10.1016/j.carbpol.2011.08.022
48. Sheltami RM, Abdullah I, Ahmad I, Dufresne A, Kargarzadeh H (2012) Extraction of cellulose nanocrystals from mengkuang leaves (Pandanus tectorius). Carbohydr Polym 88(2):772–779. doi: 10.1016/j.carbpol.2012.01.062
49. Sun Y, Cheng J (2002) Hydrolysis of lignocellulosic materials for ethanol production: A review. Bioresour Technol 83(1):1–11. doi: 10.1016/S0960-8524(01)00212-7
50. Thygesen A, Oddershede J, Lilholt H, Thomsen AB, Ståhl K (2005) On the determination of crystallinity and cellulose content in plant fibres. Cellulose 12(6):563–576. doi: 10.1007/s10570-005-9001-8
51. Segal L, Creely JJ, Martin AE, Conrad CM (1959) An Empirical Method for Estimating the Degree of Crystallinity of Native Cellulose Using the X-Ray Diffractometer. Text Res J 29(10):786–794. doi: 10.1177/004051755902901003
52. Salehi S, Noaparast M, Shafaei SZ (2016) Response surface methodology (RSM) for optimization of chalcopyrite concentrate leaching with silver-coated pyrite. Physicochem Probl Miner Process 52(2):1023–1035. doi: 10.5277/ppmp160239
53. Kasiri N, Fathi M (2018) Production of cellulose nanocrystals from pistachio shells and their application for stabilizing Pickering emulsions. Int J Biol Macromol 106:1023–1031. doi: 10.1016/j.ijbiomac.2017.08.112
54. Taflick T, Schwendler LA, Rosa SML, Bica CID, Nachtigall SMB (2017) Cellulose nanocrystals from acacia bark–Influence of solvent extraction. Int J Biol Macromol 101:553–561. doi: 10.1016/j.ijbiomac.2017.03.076
55. Mendes CADC, Ferreira NMS, Furtado CRG, De Sousa AMF (2015) Isolation and characterization of nanocrystalline cellulose from corn husk. Mater Lett 148:26–29. doi: 10.1016/j.matlet.2015.02.047

Figures

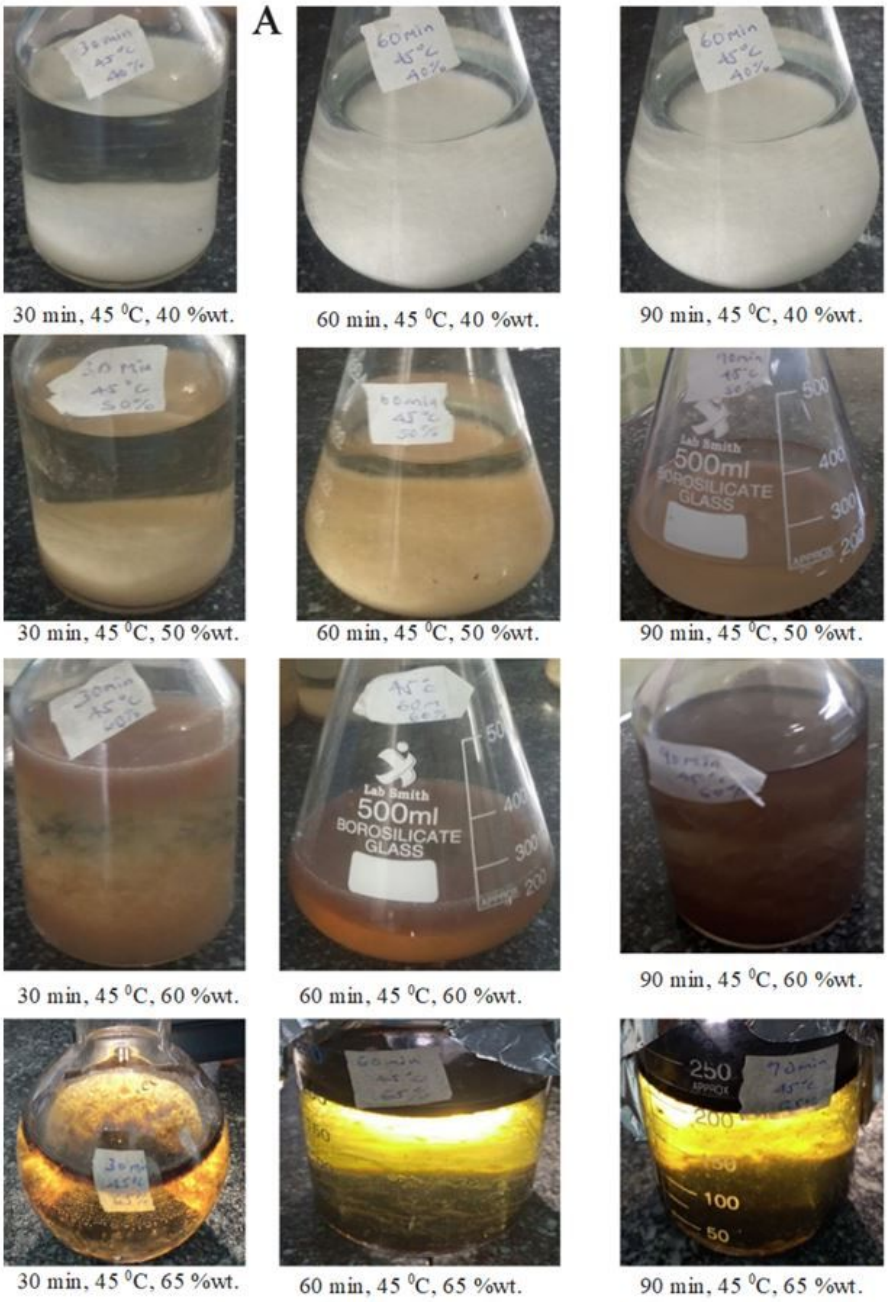

Figure 1

Summary of acid hydrolysis (A) at 45 °C hydrolysis temperature.

Figure 2

Summary of acid hydrolysis (B) at 55 °C hydrolysis temperature.

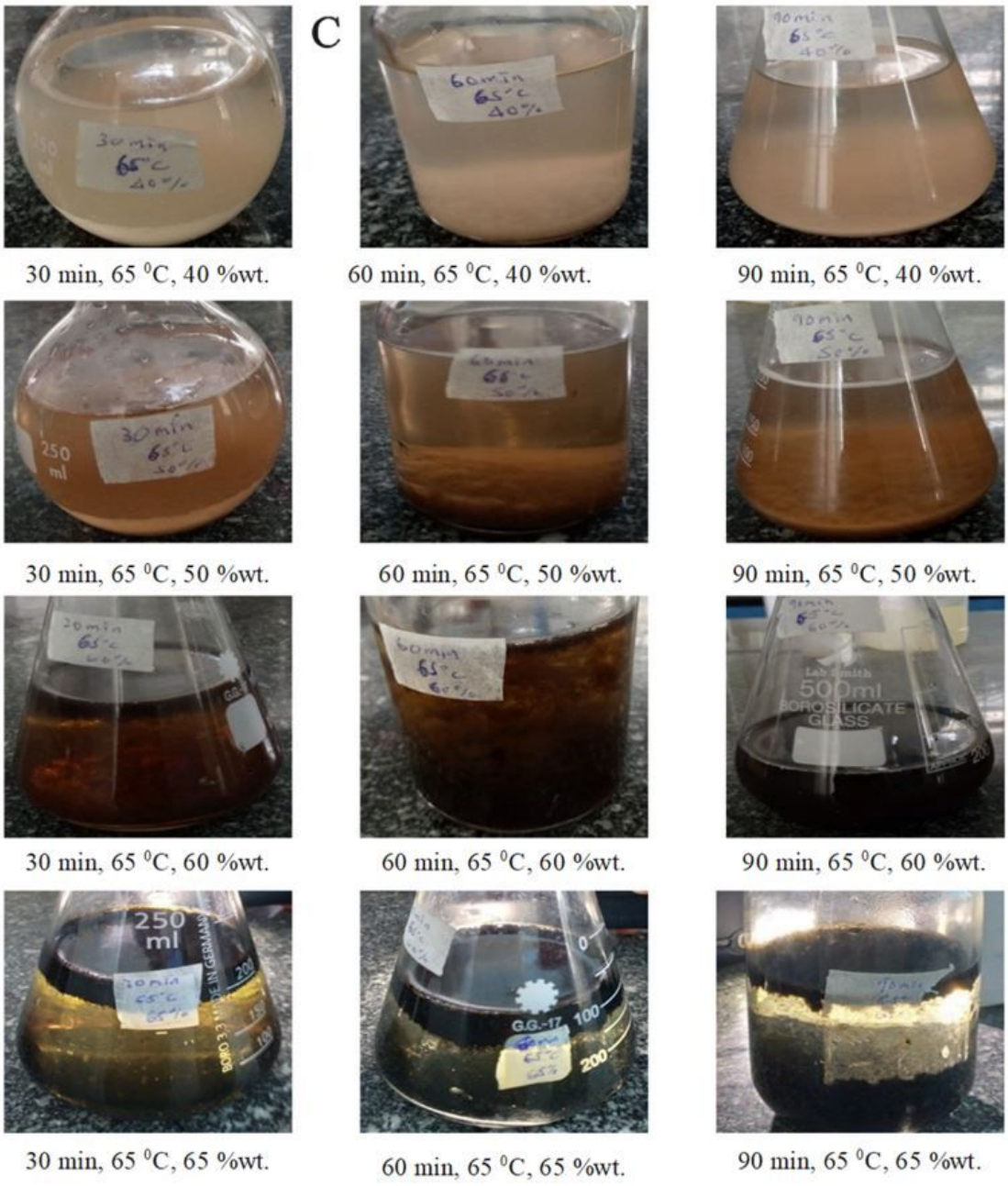

Figure 3

Summary of acid hydrolysis (C) at 65 °C hydrolysis temperature.

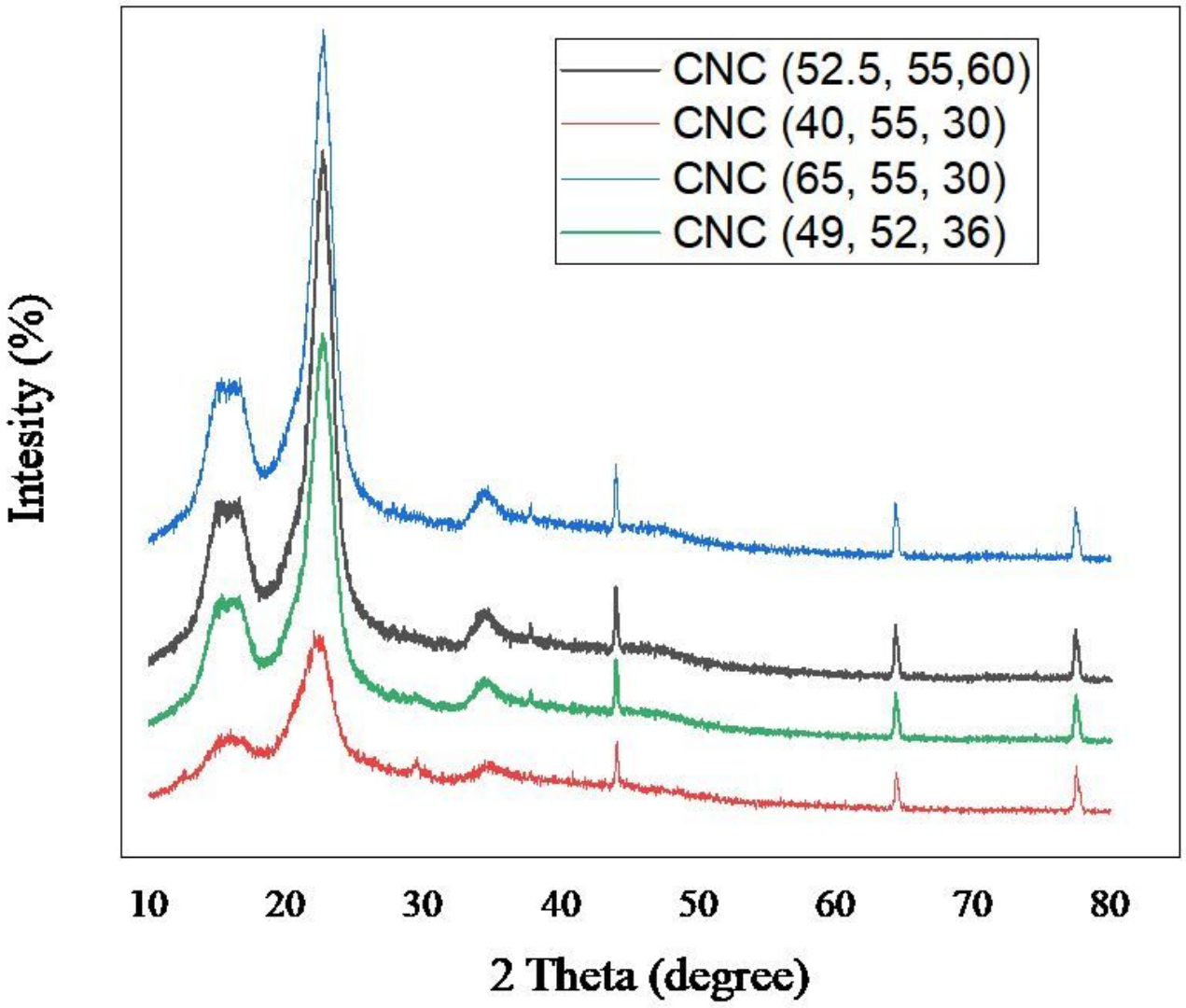

Figure 4

X-ray diffractogram investigation of the isolated cellulose nanocrystals from the pseudo stem fiber cellulose of Ensete ventricosum under various hydrolysis conditions.

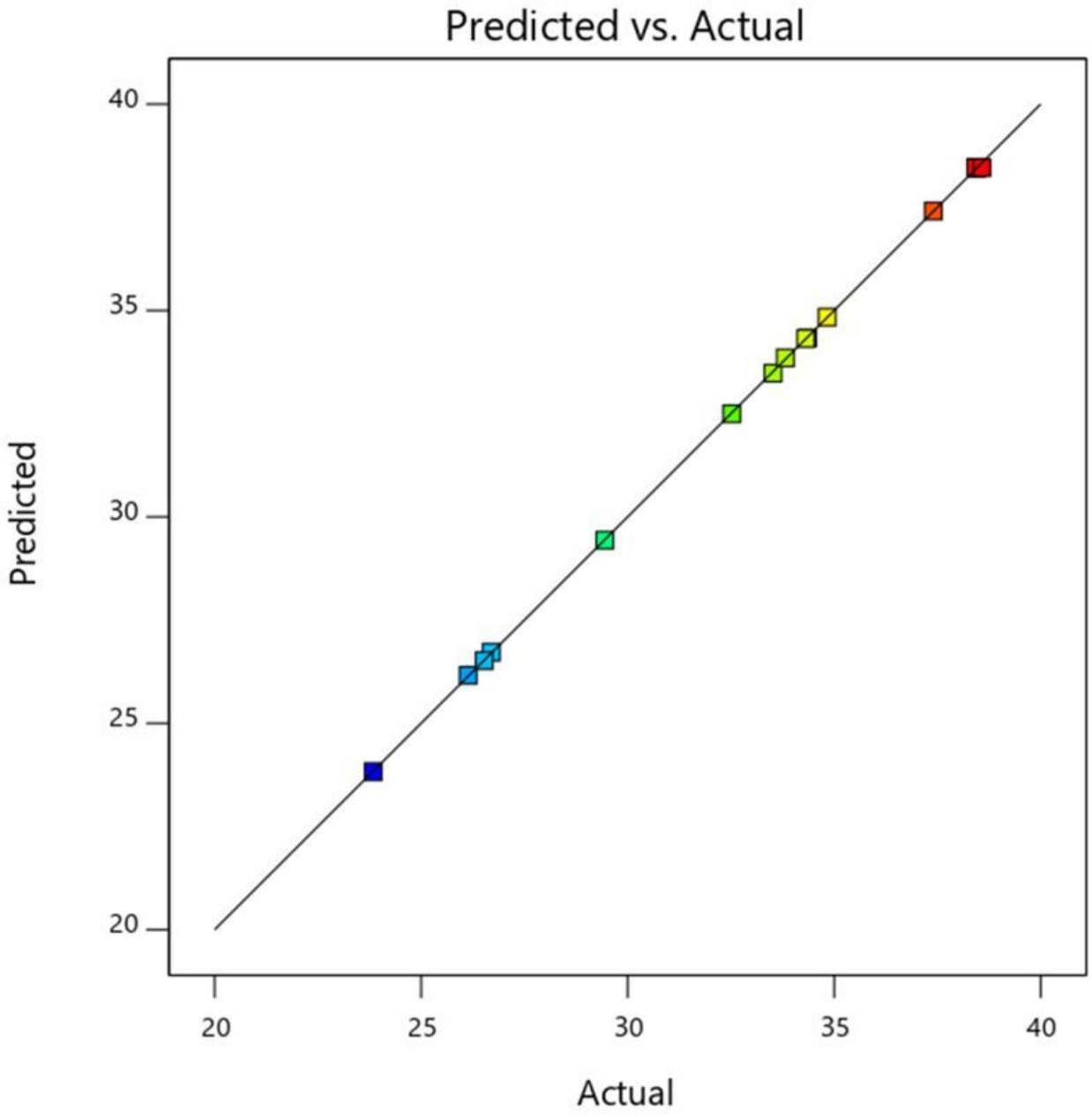

Figure 5

Normal plot of predicted Vs actual data of yield.

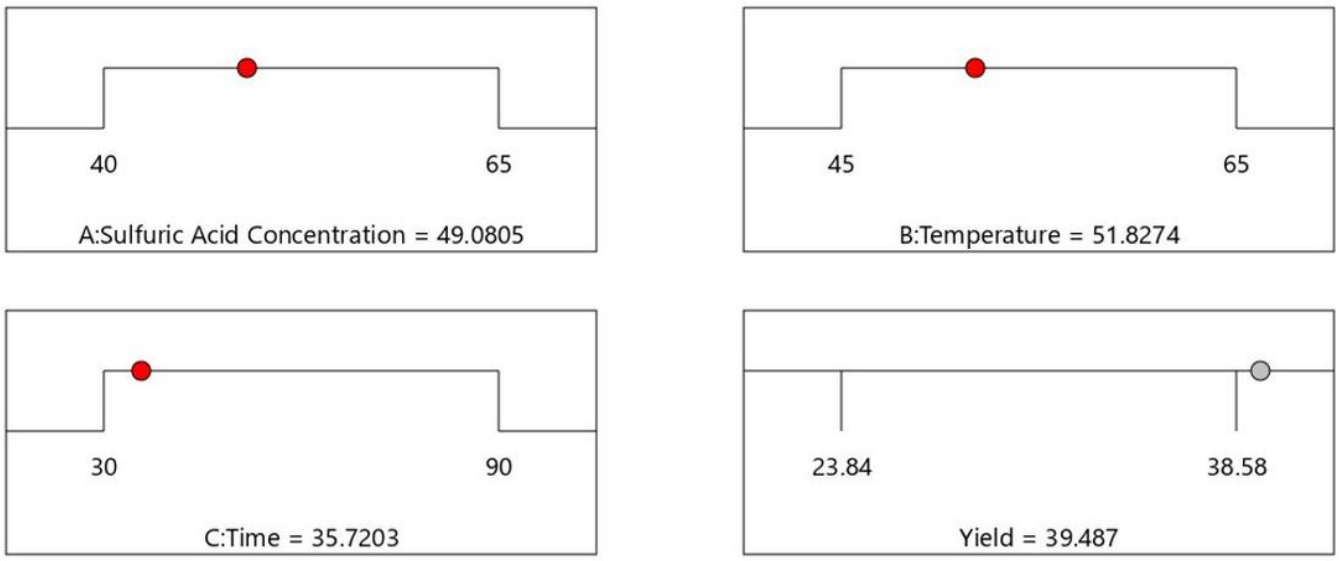

Figure 6

Expression of numerical optimization using ramps plots

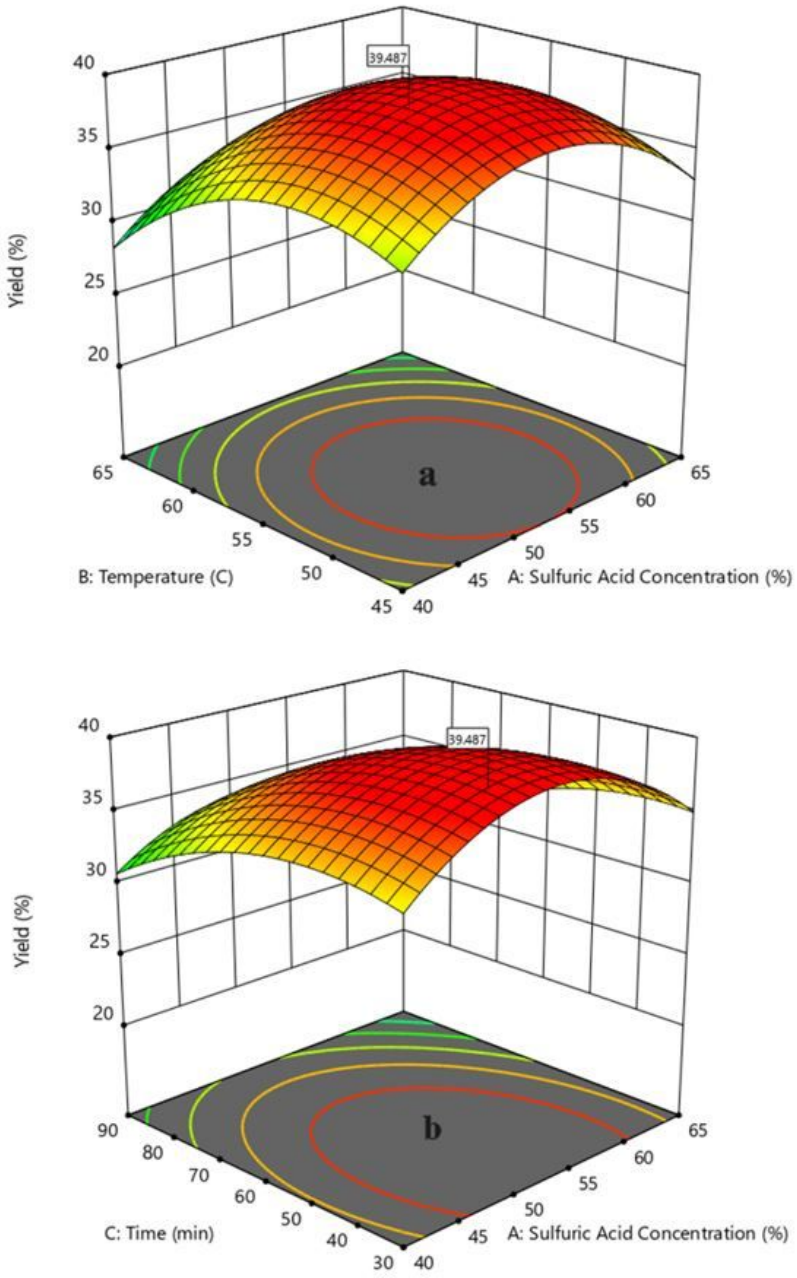

Figure 7

The surface plots for the yield (%CNCs) and effect of parameters on the yield